

Ultrafast All-Polymer Electrically Tunable Silicone Lenses

Luc Maffli, Samuel Rosset,* Michele Ghilardi, Federico Carpi, and Herbert Shea*

Dielectric elastomer actuators (DEA) are smart lightweight flexible materials integrating actuation, sensing, and structural functions. The field of DEAs has been progressing rapidly, with actuation strains of over 300% reported, and many application concepts demonstrated. However many DEAs are slow, exhibit large viscoelastic drift, and have short lifetimes, due principally to the use of acrylic elastomer membranes and carbon grease electrodes applied by hand. Here a DEA-driven tunable lens, the world's fastest capable of holding a stable focal length, is presented. By using low-loss silicone elastomers rather than acrylics, a settling time shorter than 175 μ s is obtained for a 20% change in focal length. The silicone-based lenses show a bandwidth 3 orders of magnitude higher compared to lenses of the same geometry fabricated from the acrylic elastomer. Stretchable electrodes, a carbon black and silicone composite, are precisely patterned by pad-printing and subsequently cross-linked, enabling strong adhesion to the elastomer and excellent resistance to abrasion. The lenses operate for over 400 million cycles without degradation, and show no change after more than two years of storage. This lens demonstrates the unmatched combination of strain, speed, and stability that DEAs can achieve, paving the way for complex fast soft machines.

1. Introduction

Soft actuators enable many applications and features that are not feasible with conventional approaches based on hard materials. For example, soft robots can adapt their body shape and crawl through small openings^[1] or conform to complex shapes,^[2] deformable cell culture systems can be used to strain biological cells and study mechanotransduction,^[3] and tunable optical systems based on soft and deformable materials lead to lightweight and compact adaptive systems.^[4,5] However, most existing soft actuators present serious limitations such as slow response speed, short lifetime, or must be tethered to

external bulky controllers that cannot be integrated, as is typically the case of pneumatic actuation.

In this contribution, we present a soft tunable lens with integrated electrostatic actuation, capable of changing its focal length by more than 20% in less than 175 μ s and stable for hundreds of millions of cycles. The concept is based on the bio-inspired and dielectric elastomer actuators (DEA)-driven design introduced by Carpi et al. in 2011.^[4] However, a low-mechanical loss silicone (Nusil CF19-2186) is used here as dielectric membrane, instead of acrylic elastomer. This leads to the world's fastest tunable lens with the ability to hold a very stable position, and demonstrates the integration of actuation, fast response speed, and long lifetime in a soft device. This is a nontrivial performance for a very soft system (1 MPa). For comparison, we fabricated identical lenses made of the more widely used 3M VHB acrylic elastomer, and obtained a comparable focal length tuning but with a bandwidth about 3 orders of magnitude smaller.

Among the different actuation mechanisms that have been used to drive soft actuators (pneumatic actuation,^[1] phase change,^[6] etc.), electrostatic actuation presents the advantages of being integrated into the device and consuming very little power, leading to compact, lightweight, and energy efficient devices. Charge-induced deformation of elastomeric actuators has for example been demonstrated with DEAs, which can generate very large strains, larger than 100%.^[7,8] However, most of DEAs are based on an acrylic elastomer material with a high mechanical loss factor (VHB from 3M), as this allows for the largest reported strains. Using this acrylic elastomer leads to devices that react slowly to a voltage step input, with a pronounced viscoelastic creep, which causes the strain to keep increasing over several minutes.^[9] In addition, DEAs require compliant electrodes, i.e., electrodes that can stretch as much as the device itself.^[7] Although different approaches have been developed for the stretchable electrodes, many of today's devices use carbon grease or loose carbon powder electrodes, as they can easily be manually applied.^[10] However, such electrodes are sensitive to mechanical abrasion and subject to wear, leading to devices with a short lifetime, not to mention the difficulty of precisely patterning them on a sub-millimeter level.

The compliant electrodes we use consist of a mixture of carbon black and silicone, and are precisely patterned by pad-printing with subsequent cross-linking in an oven. The process

Dr. L. Maffli, Dr. S. Rosset, Prof. H. Shea
Microsystems for Space Technologies Laboratory
École Polytechnique Fédérale de Lausanne
2002 Neuchâtel, Switzerland
E-mail: samuel.rosset@a3.epfl.ch;
herbert.shea@epfl.ch

M. Ghilardi, Prof. F. Carpi
Soft Matter Artificial Muscles & Transducers Group
Queen Mary University of London
London, E1 4NS, UK

Prof. F. Carpi
Beijing University of Chemical Technology
Beijing, China

DOI: 10.1002/adfm.201403942



forms solid electrodes with a strong adhesion to the dielectric membrane (Figure S1, Supporting Information) and an excellent resistance to mechanical abrasion and wear, leading to reproducible devices with long lifetime.

Because of their large actuation strain, DEAs are particularly interesting in the field of adaptive optics.^[5] Deformable optical lenses with electrically controllable focus present numerous advantages over the traditional approach consisting in translating rigid lenses. They have a much reduced mass and footprint, and can potentially be much faster due to the lower inertia of the system. The new DEA-based tunable lens presented here provides the advantages of being extremely fast, energy-efficient, and compact, and having a drift-free actuation. The extremely high speed and low level of viscoelastic drift demonstrated here are important requirements for tunable lenses, which have never been obtained with any other polymer so far.

The following sections present the lens design and the characterization of its electromechanical response.

2. Lens Design and Principle

The lens, based on the biomimetic principle presented by Carpi et al.^[4] consists of two prestretched elastomeric membranes bonded together and encapsulating a small amount (2–8 μ L) of transparent fluid at the centre, forming a lens. An annular compliant electrode is patterned by pad printing a conductive mixture of carbon black and silicone on both sides of the device, which is clamped between two rigid or flexible PCBs (Figure 1). The rigid printed circuit board (PCB) in Figure 1B serves as a mounting frame and to route the actuation voltage to the electrodes. The flexible frame demonstrated in Figure 1D allows the lens to be folded, and provides a support on which to bond contact wires.

The diameter of the optical lens at the centre is 5 mm, and the outer diameter of the annular electrode is 19 mm. When a voltage is applied between the electrodes, their in-plane expansion compresses the lens. Because the volume of the encapsulated liquid remains constant, this causes a decrease of the radius of curvature of the lens, and hence a decrease of its focal length. The initial focal length of the device depends on the volume of liquid encapsulated between the two membranes, with more liquid leading to a shorter initial focal length due to the larger initial curvature of the lens.

The fluid used to fill the lens must be chosen carefully, as it must fulfill optical criteria (high optical transmittance, low scattering, high index of refraction, thermal stability, durability, etc.), and at the same time be compatible with the elastomeric membrane (i.e. the fluid should not penetrate or interact with the membrane), and not evaporate through the membrane. Because of the design of the lens, the same membrane is used as dielectric for the actuator and as membrane encapsulating the liquid. In order to increase the device's tuning speed, we choose silicone membranes for the actuator,^[11] and hence also for the lens. However, silicone elastomers are gas permeable, and swell when in contact with many nonpolar liquids. Polar solvents, such as water, glycerol, and ethylene glycol, are generally considered to be compatible with polydimethylsiloxane

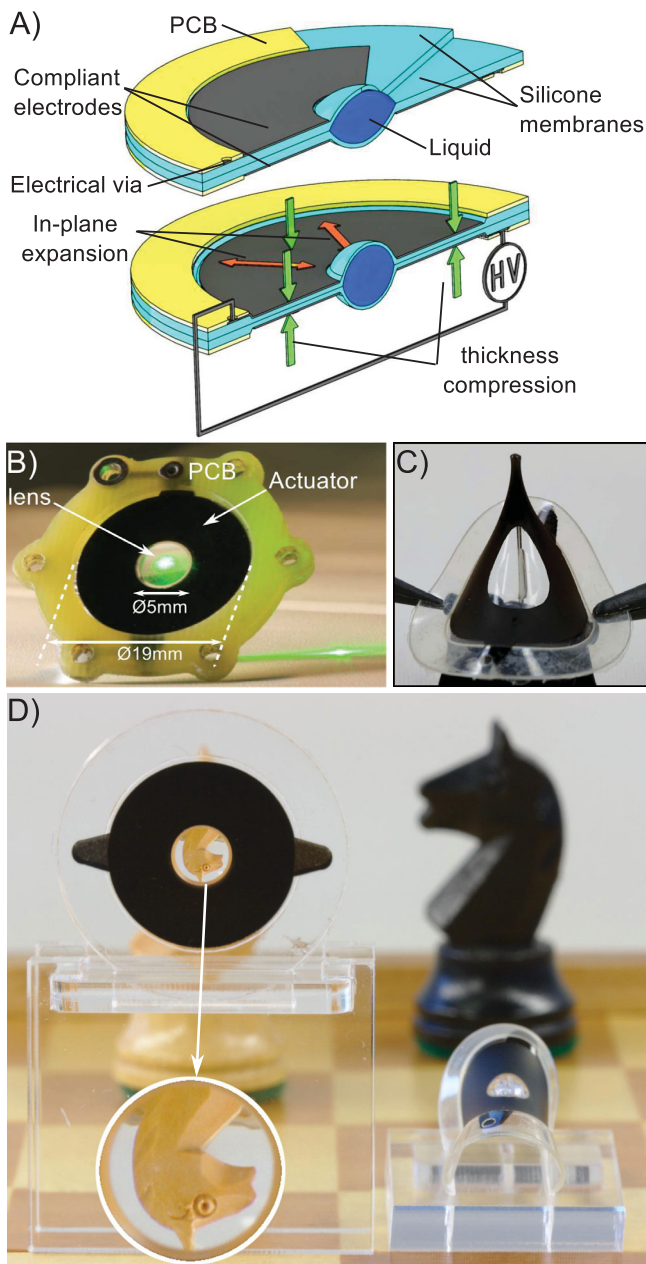


Figure 1. A) Schematic of the fast tunable DEA-driven lens, consisting of two prestretched elastomer membranes bonded together and encapsulating a transparent fluid, forming a biconvex lens. An annular compliant electrode is patterned around the lens. Upon applying a voltage, the expansion of the electrode due to Maxwell pressure compresses the lens in-plane, thus decreasing its radius of curvature and hence focal length. B) Picture of the device showing the lens at the centre, the annular electrode (black), and the outer frame. C) The resilience of the actuator is shown by an extreme deformation of the lens over a needle head. D) Flexible version of the lens revealing the white knight of a chess set hidden behind (left). The inset shows a blown-up image of the lens. The details of the knight are clearly visible. In this flexible configuration, the lens can be folded by over 180° without damage (right).

(PDMS) because they do not induce swelling of the material.^[12] However, they are not suitable for this lens because they would evaporate or diffuse through the membrane. We found that the

Sylgard 184 silicone prepolymer, used by Carpi et al. for a tunable lens based on a VHB acrylic elastomer membrane,^[4] was also the best choice for silicone membranes.^[13] The index of refraction was measured to be 1.41. Lenses made by encapsulating Sylgard 184 prepolymer have shown no volume decrease and no droplet formation on the surface of the membrane more than two years after fabrication.

We used oxygen plasma activation to bond the two silicone membranes together without the need for an adhesive or glue, to ensure the fastest possible response. Exposing silicone surfaces to low-power oxygen plasma renders them rich in O–H groups, leading to strong, irreversible covalent bonding when two treated surfaces are placed in contact.^[14] This approach has enabled us to reliably and reproducibly encapsulate the liquid between two thin silicone membranes. Details about the fabrication process of the lens are given in the Experimental Section.

The change in focal length is driven by a DEA located around the lens (Figure 1). When a voltage is applied between the electrodes of a DEA, it generates a compressive stress (Maxwell pressure) in the dielectric elastomer, which compresses the structure and reduces the membrane thickness while increasing the surface area of the electrodes. The relation between the applied voltage V and the Maxwell pressure p is given by^[7]

$$p = \epsilon_0 \epsilon_r \frac{V^2}{d^2} \quad (1)$$

where ϵ_0 and ϵ_r are, respectively, the vacuum permittivity and the relative permittivity of the dielectric, and d the thickness of the membrane. To a first approximation, assuming that the elastomer behaves as a linear elastic body, the relation between the electrostatic pressure and the strain of the electrode is inversely proportional to the Young's modulus of the elastomer. More complete models exist, which include the nonlinear mechanical behavior of elastomers.^[15] A detailed analytical analysis of the relation between the applied voltage and the steady-state radius of curvature of the lens for the device geometry we are considering here was recently published^[16] and can serve as a design tool in order to optimize the lens.

The focal length and tuning range depend on the initial filling of the lens, and on the different failure modes of the DEA. To show this graphically, we plot the focal length versus initial lens volume and diameter in Figure 2. For illustration, we plot up to 10% radial compression of the lens due to an applied voltage (i.e., the initial radius r_{off} of 2.5 mm is reduced to $r_{\text{on}} = 2.25$ mm due to an applied voltage). We compute the focal length f for different volumes of encapsulated liquid using the thin lens equation

$$\frac{1}{f} = (n-1) \left(\frac{1}{R_1} - \frac{1}{R_2} \right) \quad (2)$$

where R_1 and R_2 are the radius of curvature of the two sides of the lens. For the initial calculations, we set $R_1 = -R_2 = R$, as the two membranes have identical thickness and are equally pre-stretched. The relation between the radius of the lens r and the radius of curvature of the membrane R is obtained by solving the equation describing the volume of a spherical cap for a

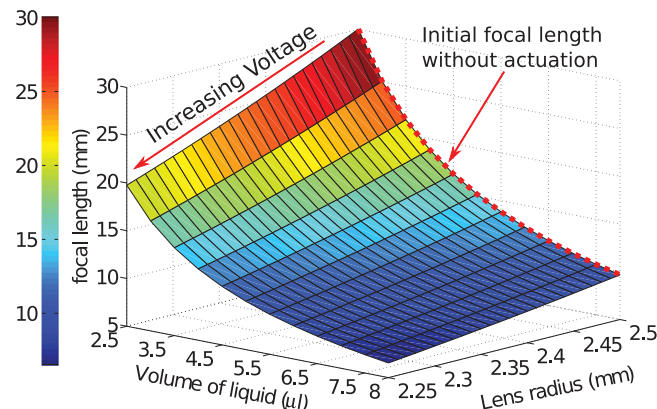


Figure 2. Computed focal length as a function of volume of liquid encapsulated in the lens, and the lens radius, which is controlled by the DEA. Because the electrostatic actuation reduces the radius of the lens, its effect on the focal length can be determined by following a line with a constant volume of liquid. The biggest voltage-induced variation of the focal length occurs for lenses with a small amount of liquid.

fixed total volume, representing the amount of liquid enclosed in the lens.

The dashed red line in Figure 2 at a constant lens radius of 2.5 mm shows the initial focal length with no actuation. It decreases for an increasing amount of liquid, i.e., for increasingly bulged lenses. The effect of voltage can be observed by recalling that the electrostatic actuation squeezes the lens and reduces its size: following a line with a constant volume of liquid, from the initial radius of 2.5 mm toward 2.25 mm (in this simplified case where we assume only up to 10% electrostatic compression), one sees clearly the decrease in focal length induced by actuation. The tuning range of the focal length depends strongly on the amount of liquid: it is larger for lenses filled with a smaller amount of liquid (i.e., with a large initial radius of curvature). The focal length changes nearly linearly with the lens diameter, and as per (1) we therefore expect a quadratic relationship between the focal length and the applied voltage.

3. Static Focal Length

The measured steady-state (DC) focal length as a function of the applied voltage is shown in Figure 3 for six different lenses (5 with a silicone membrane, and 1 with a VHB acrylic elastomer membrane), each with a different amount of liquid encapsulated between the membranes, i.e., a different initial focal length. In accordance with the theory (Figure 2), the lens with the highest initial focal length presents the highest absolute tuning range (7.1 mm), which decreases for lenses filled with more liquid. The relative tuning range of the five silicone lenses is between –26% and –19%. For comparison, we also characterized the static focal length of an acrylic elastomer-based lens of identical geometry and have obtained a maximal change of focal length of –37%. The increased tuning range compared to the silicone lenses is mainly due to the higher electric field that could be applied before breakdown, as shown in Figure 3.

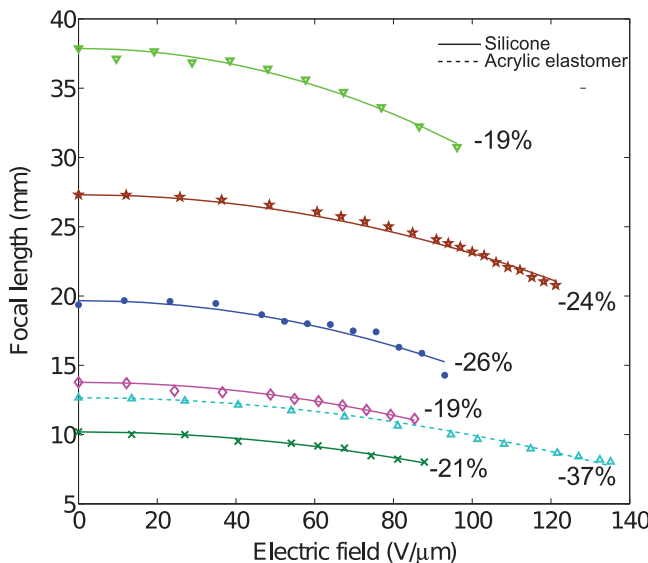


Figure 3. Measured focal length of the tunable lens as a function of electric field for different volumes of encapsulated liquid. Less liquid leads to a higher initial focal length and a larger absolute tuning range. All the tested lenses were made with silicone elastomer, except for one acrylic elastomer-based lens used as comparison (dashed line). The relative tuning ranges at the maximal voltage are indicated on the graph and lie between -26% and -19% for silicone lenses, 37% for the acrylic elastomer lens. A quadratic relationship between the electric field and the focal length has been fitted to the data points.

The focal length values that we measured directly (as described in the Experimental Section) were validated by comparison with the focal length calculated from the measured 3D shape of the actuated lenses. The shape of both sides of a test lens is measured with a white light interferometer and fitted to a sphere to obtain their radii of curvature (26.1 and 20.9 mm for top and bottom). Using the thin lens formula (2) and a refractive index of 1.41 for the liquid, we obtain a focal length of 28.3 mm, while the value recorded by our focal length setup is 29.3 mm, a very good agreement.

The white light interferometry measurement of the surface of the lens shows a non-negligible difference in the curvature radius between the top and bottom membranes. This is due to the fabrication process (cf. Section 8), and more precisely during the liquid encapsulation step, when one of the two membranes is pulled by vacuum into a spherical cavity. Because of the stretch-induced softening (Mullins effect),^[17] this membrane ends up being softer than the other, thus leading to a smaller radius of curvature when the lens is inflated with the fluid. Any deformation of the membrane during the fabrication process can have a detrimental influence on the lens quality, particularly if the deformation is not axisymmetric, as it can lead to serious astigmatism, the lens taking the shape of an ellipsoid instead of a spherical cap. The deformation induced during the liquid encapsulation is axisymmetric and therefore does not cause astigmatism. However, undesired nonsymmetric stretching of the membranes can be induced during their fabrication, when they are separated from the substrate on which they were casted. Indeed, pulling the membrane leads to very directional stretching during the release process. To avoid

such an undesired mechanical deformation during this step, we cast our membranes on substrates which were previously coated with a sacrificial layer, thus allowing for a stress-free separation of the membrane from its casting substrate by dissolution of the sacrificial layer.

The optical quality of silicone lenses is measured by phase shift interferometry at different driving electric fields. The Zernike coefficient and Strehl ratio are extracted from the data (Figure S2, Supporting Information), and show a very good optical quality up to a field of $100 \text{ V } \mu\text{m}^{-1}$ (less than $0.1 \mu\text{m}$ deviation), above which the first order astigmatism quickly increases, probably due to loss of tension in the material. As a general trend, aberrations tend to increase with increasing voltage. For driving fields smaller than $100 \text{ V } \mu\text{m}^{-1}$, the Strehl ratio is higher than 0.8, which is usually regarded as good for high quality optical systems, making these soft tunable lenses suitable for imaging applications.

The ability to electrically control the focal point of the soft lens is further demonstrated by mounting a tunable lens in front of a 5 MP charged-coupled device (CCD) imaging sensor; the tunable lens being the only optical element in front of the CCD. The spacing between the CCD and the lens is chosen so that objects far away from the lens appear in focus when no voltage is applied to the device. A $10 \text{ mm} \times 3 \text{ mm}$ EPFL (école polytechnique fédérale de Lausanne) logo is positioned at 120 mm in front of the lens, and a building located about 70 m away from the lens is also visible in the field of view (Figure 4). An applied voltage of 2.8 kV allows bringing the EPFL logo in focus, the background appearing blurry. When no voltage is applied, the situation is reversed with the background being in focus, and the logo being out of focus. At 3.5 kV, objects as close as 80 mm could be brought in focus.

4. Dynamic Response

To assess the response speed of the device to a voltage step, we characterize both the mechanical displacement of the electrodes, and the change of focal length of the lens. Since the response speed depends not only on mechanical parameters (displaced mass, stiffness, damping, viscoelasticity) but also on electrical parameters, we first measure the time required to transfer the electrical charges to the electrodes (electrical response time for kV signals).

We apply a 3.5 V amplitude square wave signal from a function generator with a rise time of less than 13 ns to a high-voltage amplifier (max output 4 kV) that has a slew rate faster than $150 \text{ V } \mu\text{s}^{-1}$ and a gain of 1000. If we neglect the leakage current across the dielectric membrane, the DEA actuator can be represented as a lumped series resistor-capacitor (RC) circuit, and the speed at which it can be charged is limited by the capacitance as well as by the series resistance of the electrodes. Our high-voltage amplifier provides a current monitoring output, and we integrate this signal $i(t)$ to determine the effective voltage V_i applied to the DEA capacitive component as a function of time

$$V_i(t) \propto \int i(t) dt \quad (3)$$

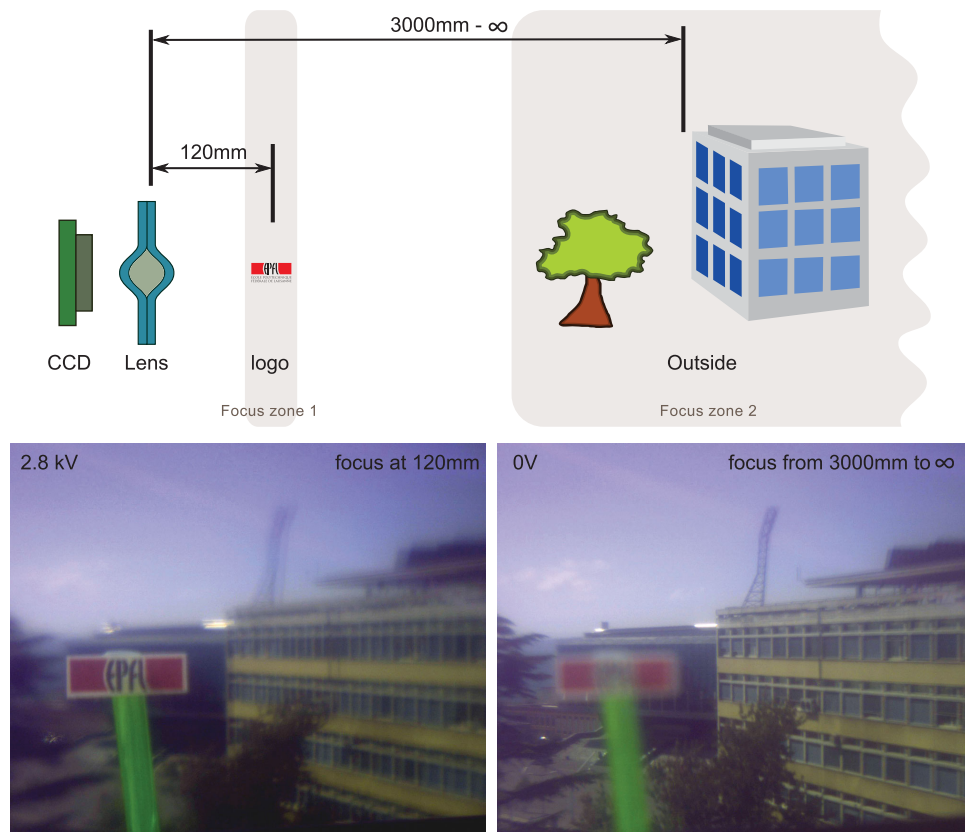


Figure 4. The tunable lens is placed directly in front of a 5 megapixel CCD sensor with no other optical elements, and used to image objects at different distances. Top: schematic representation of the setup with a 10 mm \times 3 mm EPFL logo positioned at 120 mm in front of the lens as well as trees and buildings approximately 70 m away. Bottom: resulting images captured by the sensor for 2 different driving voltages (2.8 kV, and 0V), showing the focal plane can be placed on the logo and the background.

The constant of proportionality between V_l and the integral of the current is in principle equal to the inverse of the device capacitance. However, as the capacitance has not been precisely measured and depends on the electrode strain (and is therefore time-dependent), we set the constant of proportionality so that $V_l(t \rightarrow \infty) = 3.5$ kV, i.e., the output voltage of the amplifier (Figure S3, Supporting Information).

The effective voltage applied to the capacitor, the associated displacement of the edge of the electrodes, as well as the focal length signal measured by a photodiode (cf. the Experimental Section) are reported in Figure 5 for a 3.5 kV signal with the low-voltage step applied at $t = 0$ μ s. The voltage on the electrodes takes 125 μ s to reach 90% of its steady-state value. There is a 50 μ s delay between the beginning of the voltage ramp and the onset of the electrode edge displacement. The optical signal shows stronger oscillations than the in-plane displacement of the electrodes. This is due to the shockwave sent through the liquid by the rapid expansion of the electrodes and which causes the lens to vibrate, as we observed by filming a side view of the lens with a high-speed camera. Despite these oscillations, the system is sufficiently damped so that less than 175 μ s after the start of the voltage step, the optical signal lies within $\pm 10\%$ of its final value. This makes this soft device the fastest reported tunable lens capable of holding a stable focal position. To highlight the importance of the elastomer material on the dynamic

performance, we also characterize the optical response to a voltage step of an acrylic elastomer-based tunable lens of identical dimensions. The response is strongly overdamped, shows

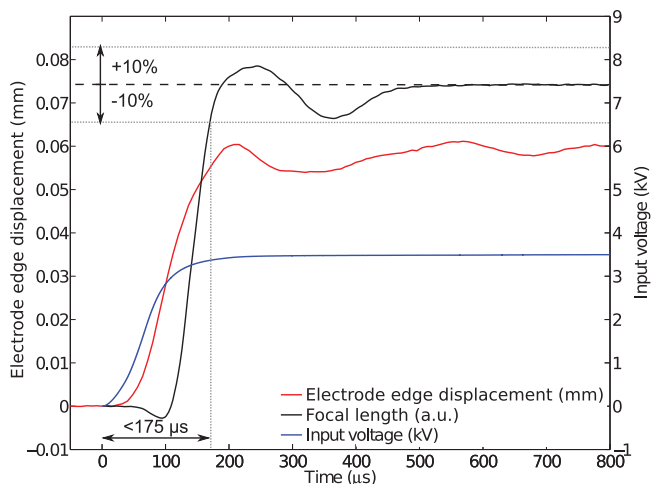


Figure 5. Electromechanical and optical response of the silicone DEA lens to a 3.5 kV voltage step input. The voltage on the electrodes takes 125 μ s to reach 90% of its final value, and the optical settling time of the system is shorter than 175 μ s.

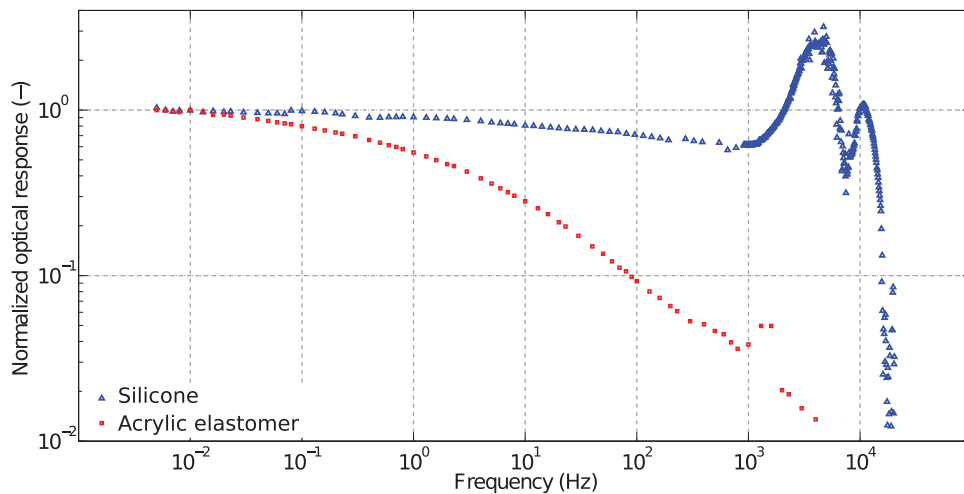


Figure 6. Frequency response of the tunable lens to large drive signals (1.4 kV), comparing silicone-based (blue triangles) and acrylic elastomer-based (red squares) lenses of identical geometry and size. The relative amplitude of the optical signal recorded on the photodiode is plotted versus frequency for excitation signals from 5 mHz to 20 kHz. The response is normalized to 1 at 5 mHz for both lenses. For the silicone lens, the response is nearly flat until the resonance peak with maximum amplitude at 4.7 kHz, allowing full tuning up to 1 kHz. For acrylic elastomer, the response drops off very quickly with frequency, limiting the acrylic elastomer lens to applications below a few Hz.

no oscillations, and has a viscoelastic drift of at least several minutes. The response clearly shows different time constants and is fitted with a 5-terms Prony series.^[9] The fastest time constant is 23 ms, but has a relative amplitude of 43% of the total response. It takes 16 s to reach 90% of the full response, which is almost five orders of magnitude slower than the settling time of the silicone-based lens.

The speed at which the focal length can be shifted between two positions has also been observed directly by shining a collimated laser beam through the lens, and inside a colloidal liquid. A high-speed camera was positioned above the bath, acquiring images at 40 000 frames per seconds (cf. Supporting Information). The shift of the focal point as observed on the movie is in agreement with the signal from the photodiode, and a stable position is reached within 400 μ s of the voltage step.

The response speed of the device can be limited by two main factors: (1) the viscoelastic properties of the electrode–elastomer–electrode sandwich that forms the actuator; and (2) the damping induced by the lens through the displacement of the liquid. To assess the importance of these two contributions, we fabricated a dummy device similar to the tunable lens, except that we did not fill the central part with the optical liquid. We measured the electromechanical displacement of the electrode edge in response to a voltage step input and obtained a rise time identical to that of the full functional lens. This result shows that the lens itself plays a negligible role in the response speed, which is dominated by the viscoelastic properties of the elastomeric actuator. Therefore, a careful choice of the silicone used as membrane material (in terms of minimization of the viscous component) could therefore lead to even faster devices.

5. Frequency Response

To further characterize the dynamic behavior of the lens, we performed a frequency response analysis of silicone-based

lenses and acrylic elastomer-based lenses, both of identical geometry and size, and made using the pad-printed carbon–silicone electrodes. A large-signal sinusoidal excitation waveform with peak-to-peak amplitude of 1400 V is used to drive the lens, which is mounted on the same setup used to characterize the dynamic response to a voltage step (cf. Section 4). The normalized amplitude of the photodiode signal is plotted as a function of the excitation frequency (Figure 6).

For the silicone-based lens, the frequency response shows an almost flat response from 5 mHz up to about 1 kHz, followed by the resonance peak at 4.7 kHz, with a relative amplitude of 3. The silicone lens can therefore follow any input signal with a bandwidth smaller than 1 kHz, which is outstanding for an actuator entirely based on soft materials, and clearly lies in a different ballpark compared to acrylic elastomer-based actuators. As shown in Figure 6, the acrylic elastomer device shows an optical response amplitude that decreases strongly with frequency. One can note a barely visible resonance at 1 kHz for the acrylic elastomer device. With 1 kHz of useable bandwidth for full-amplitude signals, the silicone-based tunable lens presented here is more than 3 orders of magnitude faster than devices made with acrylic elastomer.

Few articles report detailed characterization of the frequency response for acrylic elastomer-based DEAs. Among them, Molberg et al. have shown a constantly and rapidly decreasing strain amplitude for frequencies ranging from 10⁻³ to 1 Hz,^[18] an observation also reported by Keplinger et al. between 0.04 and 1000 Hz (displacement roughly 100 times smaller at 1 kHz than at 0.04 Hz).^[19] The acrylic elastomer VHB has a very high mechanical loss tangent, increasing from 0.3 to almost 1 in the 1 mHz to 100 Hz frequency range.^[18] Molberg et al. observed that although at very low frequencies acrylic elastomer-based devices lead to larger strains compared to silicone devices, the strain of their silicone actuators was larger than acrylic elastomer (VHB) actuators for frequencies above 0.1 Hz.

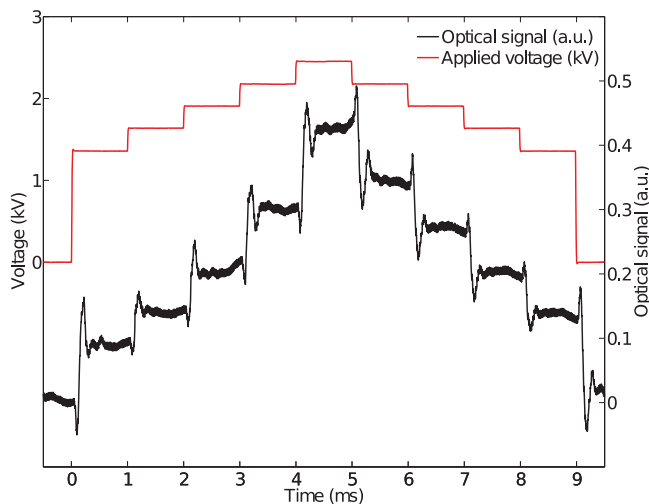


Figure 7. Optical response of the silicone lens to voltage steps of increasing amplitude with 1 ms of holding time per step. The lens is able to follow the step and stabilize during the short holding time, allowing thousands of different stable focal lengths to be generated per second.

To further demonstrate the capability of our silicone-based lens to follow a 1 kHz signal, we drive it with a series of steps of increasing voltage (0, 1.3, 1.6, 1.9, 2.2, 2.5 kV and down), with holding time of 1 ms at each step. We record the amplitude of the optical signal using the same setup used for the step response (cf. Section 4). Despite the very short holding time, the lens is fast enough to shift its focal length and stabilize within the 1 ms step duration (Figure 7).

6. Discussion

The very short settling time of the lens (<175 μ s) is mainly due to two important factors: (1) the use of silicone as a dielectric membrane for the actuator; and (2) the overall design of the lens, which minimizes the damping and inertia of the moving masses.

The response speed of the actuator is mainly dominated by the properties of the elastomer used as membrane. In this work, we have used a commercial silicone (CF19-2186 from Nusil) amongst many available products with different properties in terms of Young's modulus, mechanical loss factor, and dielectric breakdown field, which have a direct influence on the behavior of the actuator. Silicones with a higher Young's modulus generally have a lower mechanical loss tangent, but being stiffer, have lower actuation strain. The Young's modulus of the silicone used for the lens was determined from a uniaxial pull-test on a 30 μ m-thick test sample. The data were fitted with a Yeoh hyperelastic model, and the Young's modulus calculated from the parameter C_1 was 0.78 MPa. The hardness of this silicone places it at the higher end of silicones typically used for DEAs (Young's modulus between 0.1 and 1 MPa), and it therefore enters into the category of harder silicones with lower mechanical loss tangent. Despite its relatively high Young's modulus for a PDMS, the lenses made with this material exhibit the same tuning range shown by similar devices made by Carpi et al. with the acrylic elastomer VHB,^[4] a finding

which is confirmed by our own characterization of acrylic elastomer-based lenses. This shows that the use of silicone allows for gaining several orders of magnitude in response speed, without sacrificing much tuning range. The response speed of the actuator can also be influenced by the electrodes, which can contribute to the viscoelasticity of the device. For example, Rosset et al. have shown that the rise time of actuators made with 3 different silicones (with hardness between Shore A 24 and A 5) and 3 different types of electrodes (metal ion implantation, conductive rubber, and carbon grease) is mainly influenced by the type of electrode, and not the hardness of the silicone used as dielectric.^[11] Consequently an optimization of the carbon black mixture used in this work for the compliant electrodes could further increase the response speed of the device.

One particularly interesting feature of this lens design is the very small amount of liquid that needs to be displaced upon actuation: only a small shell of fluid close to the membrane is moved during actuation, while the bulk of the fluid remains still at the centre of the lens. Consequently, the contribution of the fluid to the response speed of the device is negligible, and the DEA remains the dominant part, as observed in the dynamic measurement with a full lens and a dummy device without liquid (cf. Section 4).

In addition to the remarkable achieved response speed, the implemented fabrication process leads to the efficient fabrication of reproducible devices, which exhibit long lifetime. Unlike the widely used technique of manually smearing carbon grease over the membrane, the automated stamping method used here allows us to precisely and reproducibly pattern a mixture of carbon black and silicone on thin silicone membranes without damaging them. After the patterning step, the conductive ink is cross-linked in an oven, which provides strong adhesion of the electrode on the dielectric membrane, thus producing electrodes which are resilient, resistant to wear, and extremely stable over time. Silicone lenses were actuated at 1 kHz for more than 400 million cycles with no change in performance, and devices made more than 2 years ago are still working without performance degradation in the actuator or in the lens (no loss of optical fluid).

One drawback of the lens design used in this work is the limited achievable tuning range, which is due to the fact that the expansion of the electrodes compresses the lens radially, which increases the curvature of an already curved lens. As shown in Figure 2, the absolute achievable tuning range becomes smaller when the amount of encapsulated liquid becomes larger (i.e., larger initial curvature), thus limiting the tuning range to 19%–26% for silicone lenses and 26.4%–37% for acrylic elastomer lenses. Other DEA-based tunable lenses approaches have demonstrated a much larger tuning range. For example, Wei et al. recently reported on a lens in which an optical liquid is moved back and forth from the central lens to an annular DEA surrounding it and acting like a pump.^[20] In that design, upon activation of the DEA, the curvature of a central membrane, which serves as the lens, decreases and could in principle reach a completely flat state and therefore an infinite focal length. A tuning range of 300% has been demonstrated for that geometry. However, as the displaced fluid is forced through a channel, the fluidic impedance of this design slows down the overall response speed of the device: indeed, although the lens is also made with

a silicone membrane, a response speed of a few hundred of milliseconds is reported.^[20] So, the large tuning range comes at the cost of a slow response time. In another configuration, Shian et al. have demonstrated a liquid lens formed by two back-to-back membranes of different diameters enclosing an optical liquid. One of the membranes is coated with transparent compliant electrodes and expands upon actuation, leading to a reduced curvature in the second membrane. When the diameter of the active membrane is larger, then the reduction of curvature of the passive membrane dominates, and a large positive tuning range up to 100% can be obtained.^[5] The response speed of that lens is in the range of hundreds of millisecond,^[5] probably mostly due to the use of acrylic elastomer as dielectric membrane rather than to the effect of inertia or fluidic impedance. In that device, the mass of the displaced volume of liquid upon actuation is rather small, and consequently, it is expected that a combination of that design with low-loss silicone elastomer as dielectric would lead to considerable improvement in response speed and large tuning range.

Because of DEAs are electrostatically actuated actuation and are typically made from dielectric membranes of 10–100 μm in thickness, they generally require voltages in the range of 1–10 kV for maximum displacement (about 3 kV for the devices presented in this article). Nevertheless, the mean driving currents are very small (since only a small capacitance needs to be charged), and – neglecting the leakage through the dielectric membrane – no power is necessary to hold a static position. However, the high driving voltage can be an issue, because it makes the drive electronics more complex, and often bulky and expensive especially when high slew rates are required, as is the case to drive fast devices. One possibility to reduce the driving voltage consists in decreasing the thickness of the elastomeric membrane. However, this would reduce the lateral actuation force exerted on the central lens by its surrounding annular actuating membrane, thus also reducing the deformation of the lens and the associated change of focal length too. Stacking several membranes, one on top of each other, can compensate this effect, as it would increase the total lateral force applied to the lens. Since the actuator of our device consists of two membranes bonded together (cf. Section 8), the driving voltage could straightforwardly be divided by two by patterning an electrode at the interface between them.

7. Conclusions

Our tunable lens with a settling time shorter than 175 μs demonstrates that soft and compliant systems, and particularly dielectric elastomer actuators, can combine high strain and stretchability with a fast response time, when materials with low mechanical loss factors are used. Our silicone-based lens has the ability to change its focal length extremely rapidly, but equally importantly, it does not exhibit viscoelastic drift, thus allowing to accurately hold a stable focal position.

This position stability is very important for many applications involving tunable lenses, where it is desirable to rapidly switch between different focal lengths, and to remain at a constant focal length during image acquisition. Such ultra-fast tunable lenses can be used for high-frequency varifocal

applications such as 3D and ultra-depth-of-field imaging techniques (light sheet microscopy,^[21] quasi-simultaneous imaging of multiple focal planes,^[22] depth from focus^[23] or advanced laser machining techniques.^[24] Imaging applications that require a fast change of focal point would be particularly suited for this lens design, because they only require a small change of focal length (the 20%–25% change of focal length that we obtained is sufficient to vary the focusing distance between 80 mm and infinity when the lens is simply mounted in front of a CCD sensor, Figure 4). In addition, the lens exhibits a good optical quality (Figure S2, Supporting Information). This is made possible by smooth surfaces, a well-controlled geometry and the absence of light-scattering particles in the light path (clear optical liquid, membrane with low filler content, and no compliant electrode on the lens itself). Optical quality characterization of soft DEA-based tunable lenses has not been reported prior to this work, and this is an essential parameter for any practical imaging application.

Fast (>kHz) speed and drift-free compliant dielectric elastomer actuators are expected to find applications in many fields when compliance and speed are needed; for example, in tunable gratings for spectroscopy or telecommunication, flexible grippers,^[25] tunable mm-wave phase shifters,^[26] and many aspects of soft robotics in general.

8. Experimental Section

Silicone Membranes: We used the silicone Nusil CF19–2186 (hardness Shore A 25) as material to make the membranes, which were blade-casted on polyethylene terephthalate (PET) foils to a thickness of 30 μm .^[27] We then prestretched the membranes equibiaxially by 20%–25% using a custom stretcher with 8 movable fingers. Prestretching the membranes is necessary to avoid loss of mechanical tension in the membrane upon actuation. We computed the prestretch by measuring the thickness of the membrane before and after prestretch by white light transmission interferometry.

Compliant Electrodes: We patterned the compliant electrodes using a high-throughput commercial printing technique called pad printing, in which the desired pattern is transferred on the membrane by a soft silicone stamp, thus avoiding damaging the thin membrane (Figure 8A). The ink consisted of carbon particles (Cabot black pearls 2000) dispersed in a soft silicone matrix (Silbione LSR 4305) with a 1:10 mass ratio. After printing, we placed the membranes in an oven for 30 min at 80 °C to allow the ink to cross-link, leading to well-defined electrodes with a homogeneous thickness in the range of 1 μm .

Liquid Encapsulation: We chemically activated two identical membranes with oxygen plasma (Figure 8B). We placed one of the membranes on a vacuum chuck with a 5 mm diameter spherical-shaped cavity in its centre. The membrane is pulled into the spherical hole, and we partially filled the spherical cavity with a controlled amount of Dow Corning Sylgard 184 prepolymer using an automated dispenser. We then placed the second membrane on top of the first one and we kept the vacuum on for 45 min to allow for bonding to take place between the two activated silicone membranes brought in contact (Figure 8C). As we switched off the vacuum, the bottom part of the membrane was released, and the lens was formed. The air trapped inside the lens diffused through the silicone membrane within a few hours. We then glued one PCB on each side of the membrane, which serves both as mechanical support and electrical interconnect (Figure 8D).

VHB Lenses: The lenses made with VHB acrylic elastomer were prepared in a similar manner than the silicone lenses. VHB 4905 elastomer (3M, St. Paul, MN) was prestretched equibiaxially to an area stretch ratio of 20. The electroding and filling processes are identical

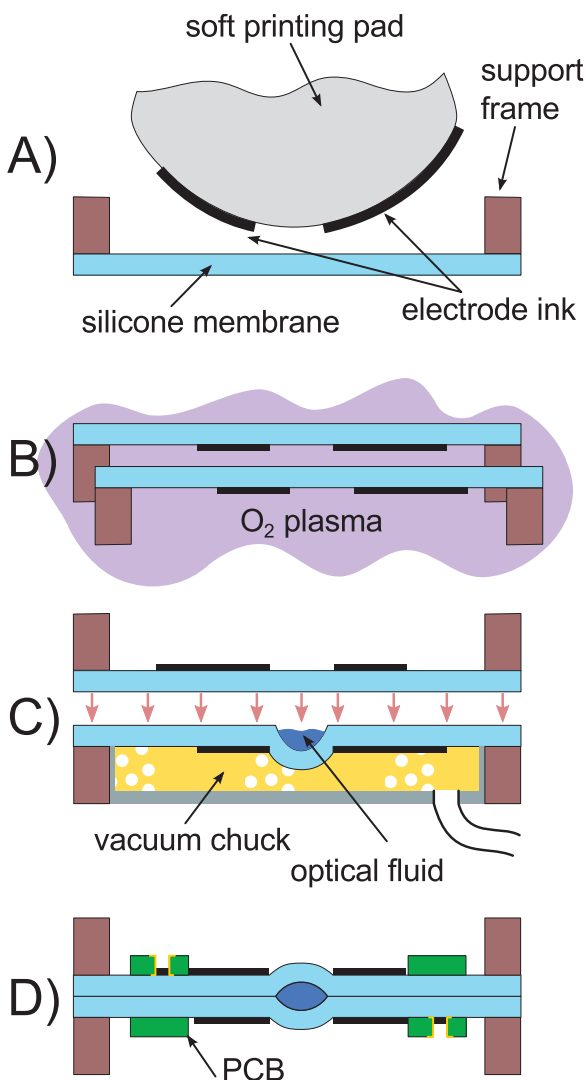


Figure 8. Fabrication process of the lens. A) Patterning by pad printing of compliant electrodes on the backside of two 15 μm -thick silicone membrane stretched on a frame. B) Short activation of the surface of the membranes with oxygen plasma. C) One membrane is placed on a vacuum chuck and vacuum is applied to create a cavity at the centre of the membrane, which is filled with a controlled amount of liquid. The second membrane is applied upside-down on the first, and the assembly is left in this position for 45 min, during which covalent bonding takes place. D) The vacuum is released and the assembly removed from the chuck. The excess of air trapped into the lens diffuses through the membrane in a matter of hours. PCBs (flexible or rigid) are applied on both sides of the membrane to ensure electrical contacts, and the holding frames are discarded.

than what is shown in Figure 8, skipping the oxygen plasma activation (step b), as we rely on the intrinsic adhesive nature of VHB to stick the two membranes together. The lens was then placed in an oven at 80 °C for 30 min, in order to improve the bonding strength between the two membranes.

Focal Length and Optical Quality Measurement: We measured the focal length by shining a collimated 633 nm He–Ne laser beam through the tunable lens, and then on a movable screen. The imaging screen, coupled to a 5 megapixel uEye camera (IDS, Germany) with a 3.3x macro objective, was mounted on a precision stage. We measured the

diameter of the laser spot as a function of the lens–screen distance, and the focal length was defined as the distance leading to the smallest spot size. The measurement was conducted for different values of applied voltage, to obtain the focal length versus voltage plot. For the lenses which were characterized by phase shift interferometry (PSI, Figure S2, Supporting Information), the focal length as a function of voltage was directly obtained from the measurement data. The PSI setup (Prof. Schwider, Erlangen, Germany) is a Mach–Zehnder interferometer with a He–Ne laser source ($\lambda = 633$ nm). The interference between a wavefront shone through the lens and a reference planar wave front is measured by a CCD camera. The smallest magnification objective is used in order to maximize the field of view (1.34 mm in diameter).

Dynamic Response: The electromechanical response of the device to a voltage step input was characterized by imaging the in-plane motion of the electrode edge with a high-speed camera Phantom V210 from Vision Research mounted on a microscope with a 20x objective. The video resolution was selected at 32 \times 160 pixels, with a frame rate of 125 kHz. A black and white threshold was performed and we converted the displacement from pixels to mm using a calibration ruler. The optical response of the device to a voltage step input was characterized by measuring the optical power density of a collimated 633 nm laser beam being shone through the lens and a pinhole, and then impacting a photodiode (Thorlabs PDA100A) with a 78 kHz bandwidth, located at a fixed distance from the lens, similar to the measurement technique used by Yu et al.^[28] For both the electromechanical and optical response, the voltage step input was generated by a function generator (Agilent 33220A) connected to a 4 kV high-voltage amplifier (Trek 609E-6). The output of the function generator is also used as a trigger signal for both the high-speed camera, and the oscilloscope recording the signal of the photodiode, in order to have precise time synchronization between the different measurements.

Frequency Response: We measured the frequency response of our lens with a large-signal sinusoidal excitation, using the same setup as for the dynamic optical response described above. The signal of the photodiode is fed to a Stanford Research SR830 lock-in amplifier. A high-voltage sinusoidal signal with a DC offset was applied to the lens. The peak-to-peak amplitude of the signal was 1400 V with a 750 V DC offset and with a frequency sweep from 0.005 Hz to 20 kHz (limited by the bandwidth of the high voltage amplifier). The optical signal was measured by the lock-in amplifier at the same frequency than the driving signal. We also measured the high-voltage amplifier's gain and phase with a load in the same conditions to remove the contribution of the amplifier from the measured data.

Supporting Information

Supporting Information is available from the Wiley Online Library or from the author.

Acknowledgements

This research was funded by the Swiss National Science Foundation, Grant No. 200020-153122 and 200020-140394, by the SNSF R'equip program Grant No. 206021-139187, and by COST – European Cooperation in Science and Technology action MP1003. The authors thank the LMTS EAP team for helpful comments and advice, as well as Dr. Toralf Scharf, EPFL-OPT, for his precious help for the PSI characterization of the lenses quality.

Received: November 7, 2014

Revised: January 6, 2015

Published online: January 23, 2015

- [1] R. F. Shepherd, F. Ilievski, W. Choi, S. A. Morin, A. A. Stokes, A. D. Mazzeo, X. Chen, M. Wang, G. M. Whitesides, *Proc. Natl. Acad. Sci. U.S.A.* **2011**, *108*, 20400.
- [2] S. Kim, C. Laschi, B. Trimmer, *Trends. Biotechnol.* **2013**, *31*, 287.

[3] Y. Zhao, J. Zhou, W. Dai, Y. Zheng, H. Wu, *J. Micromech. Microeng.* **2011**, *21*, 054017.

[4] F. Carpi, G. Frediani, S. Turco, D. De Rossi, *Adv. Funct. Mater.* **2011**, *21*, 4152.

[5] S. Shian, R. M. Diebold, D. R. Clarke, *Opt. Express* **2013**, *21*, 8669.

[6] R. Altmüller, R. Schwödauer, R. Kaltseis, S. Bauer, I. Graz, *Appl. Phys. A: Mater. Sci. Process* **2011**, *105*, 1.

[7] R. Pelnine, R. Kornbluh, Q. Pei, S. Oh, J. Joseph, *Science* **2000**, *287*, 836.

[8] C. Keplinger, T. Li, R. Baumgartner, Z. Suo, S. Bauer, *Soft Matter* **2012**, *8*, 285.

[9] M. Wissler, E. Mazza, *Smart Mater. Struct.* **2005**, *14*, 1396.

[10] S. Rosset, H. Shea, *Appl. Phys. A: Mater. Sci. Process* **2013**, *110*, 281.

[11] S. Rosset, P. Gebbers, B. M. O'Brien, H. R. Shea, *Proc. SPIE* **2012**, *8340*, 834004.

[12] J. N. Lee, C. Park, G. M. Whitesides, *Anal. Chem.* **2003**, *75*, 6544.

[13] L. Maffli, Ph.D. Thesis, École polytechnique fédérale de Lausanne (EPFL), Switzerland **2014**.

[14] S. Bhattacharya, A. Datta, J. Berg, S. Gangopadhyay, *J. Microelectromech. Syst.* **2005**, *14*, 590.

[15] Z. Suo, *Acta Mech. Solida Sin.* **2010**, *23*, 549.

[16] T. Lu, S. Cai, H. Wang, Z. Suo, *J. Appl. Phys.* **2013**, *114*, 104104.

[17] L. Mullins, *Rubber Chem. Technol.* **1969**, *42*, 339.

[18] M. Molberg, Y. Leterrier, C. J. G. Plummer, C. Walder, C. Loewe, D. M. Opris, F. A. Nuesch, S. Bauer, J.-A. E. Manson, *J. Appl. Phys.* **2009**, *106*, 054112.

[19] C. Keplinger, J.-Y. Sun, C. Foo, P. Rothemund, G. Whitesides, Z. Suo, *Science* **2013**, *341*, 984.

[20] K. Wei, N. W. Domicone, Y. Zhao, *Opt. Lett.* **2014**, *39*, 1318.

[21] F. O. Fahrnbach, F. F. Voigt, B. Schmid, F. Helmchen, J. Huisken, *Opt. Express* **2013**, *21*, 21010.

[22] M. Duocastella, B. Sun, C. B. Arnold, *J. Biomed. Opt.* **2012**, *17*, 050505.

[23] R. Rahmat, A. S. Malik, N. Kamel, H. Nisar, *J. Vis. Commun. Image R.* **2013**, *24*, 303.

[24] M. Duocastella, C. B. Arnold, *Appl. Phys. Lett.* **2013**, *102*, 061113.

[25] O. A. Araromi, I. Gavrilovich, J. Shintake, S. Rosset, M. Richard, V. Gass, H. R. Shea, *IEEE/ASME Trans. Mechatron.* **2015**, *20*, 438.

[26] P. Romano, S. Araromi, S. Rosset, H. Shea, J. Perruisseau-Carrier, *Appl. Phys. Lett.* **2014**, *104*, 024104.

[27] L. Maffli, S. Rosset, H. R. Shea, *Smart Mater. Struct.* **2013**, *22*, 104013.

[28] H. Yu, G. Zhou, F. S. Chau, S. K. Sinha, *Sens. Actuators A* **2011**, *167*, 602.